Crystal field excitations on $NdFe_3(BO_3)_4$ investigated by inelastic neutron scattering

S. Hayashida[1], M. Soda[1], S. Itoh[2], T. Yokoo[2], K. Ohgushi[3], D. Kawana[1], and T. Masuda[1]

[1]Neutron Science Laboratory, Institute for Solid State Physics, University of Tokyo, Tokai, Ibaraki 319-1106, Japan
[2]Neutron Science Division, Institute of compounds Structure Science, High Energy Accelerator Research Organization, Tsukuba, Ibaraki 305-0801, Japan
[3]Department of Physics, Tohoku University, Sendai, Miyagi 980-8581, Japan

E-mail: hayashida@issp.u-tokyo.ac.jp

Abstract. We performed inelastic neutron scattering experiments on a multiferroic material $NdFe_3(BO_3)_4$ to explore the crystal field excitations, where the magnetic anisotropy of the Nd^{3+} crystal field was responsible for the multiferroicity. Flat modes were observed at 8.5 meV and 17.4 meV in the neutron spectrum. The analysis revealed that these excitations were the transitions from the ground state to the first and second excited states of the Nd^{3+} crystal field.

1. Introduction

Multiferroic compounds, which exhibit both magnetic and dielectric orders, have attracted great attention since the discovery of a huge magnetoelectric (ME) effect in $TbMnO_3$ [1]. Among them, the rare-earth ferroborates $RFe_3(BO_3)_4$ (R = Y and rare-earth metal) are a series of new multiferroic compounds containing R^{3+} ($4f^n$) and Fe^{3+} ($3d^5$ $S = 5/2$) as magnetic ions. They show diverse ME effects as a function of the R^{3+} ions (R = Y, Pr, Nd, Sm, Gd and Tb) [2, 3, 4, 5, 6, 7] because of the variety of magnetic anisotropies and of strong coupling to the Fe^{3+} moments. Recent studies revealed that the mechanism of the magnetoelectricity in these compounds was explained by the spin-dependent metal-ligand hybridization model [8, 9].

We focus on $NdFe_3(BO_3)_4$, where the Nd^{3+} ions ($4f^3$) carry a magnetic moment with $J = 9/2$. The crystal structure of $NdFe_3(BO_3)_4$ is trigonal with space group $R32$. The point symmetry of the NdO_6 octrahedra is D_3; a threefold symmetry along the crystallographic c - axis and three twofold axes in the ab - plane as shown in Fig. 1(a). Studies on the heat capacity, magnetic susceptibility [10], and ME effect [3, 6] revealed that an easy-plane type antiferromagnetic (AF) order and a spontaneous electric polarization simultaneously appeared at T_N = 30 K and a huge electric polarization was induced by a magnetic field. An optical spectroscopy study exhibited five Kramers doublets by the Nd^{3+} crystal field [11]. A neutron diffraction study exhibited the easy-plane type AF order at $T \leq T_N$; the Fe^{3+} and Nd^{3+} magnetic moments aligned ferromagnetically along the a - axis and aligned antiferromagnetically along the c - axis with the propagation vector $\boldsymbol{k}$ = (0, 0, 3/2) [12, 13].

In the present study we explored the crystal field excitations of the Nd^{3+} ion in $NdFe_3(^{11}BO_3)_4$ by means of an inelastic neutron scattering (INS) technique. Very recently it

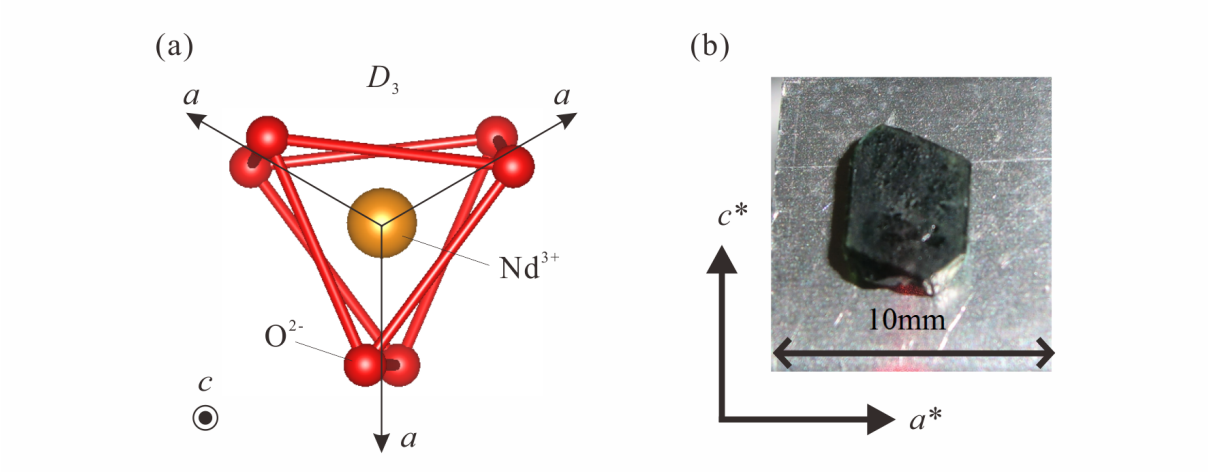

Figure 1. (a) The ab - plane projection of the NdO_6 octahedra in the D_3 symmetry. (b) A single crystal of $NdFe_3(^{11}BO_3)_4$

was revealed that the magnetic anisotropy of the Nd^{3+} crystal field drove the multiferroicity in $NdFe_3(BO_3)_4$ [14]. It is significant to investigate the Nd^{3+} crystal field for the further understanding of the ME effect in the rare-earth ferroborates.

2. Experimental details

Single crystals of $NdFe_3(^{11}BO_3)_4$ were grown by a flux method [15]. Details of the growing method are described in Ref. [14]. Plate-shaped crystals having the crystallographic a^*-c^* plane as shown in Fig. 1(b) were obtained. 22 pieces of the single crystals were coaligned so that the a^*-c^* plane was horizontal. The crystal alignment was performed by a transmission Laue method using a high energy X-ray CCD camera. We placed the crystals on an aluminum holder. The average mass of the crystals was 0.1 g. The total mass of the sample was 2.1 g.

We performed the INS experiment at the High Resolution Chopper Spectrometer (HRC) installed in the Material and Life Science Experimental Facility of J-PARC [16, 17, 18]. White neutrons are monochromatized by a Fermi chopper synchronized with the production timing of the pulsed neutrons at the HRC. The energy transfer $\hbar\omega$ was determined from the time of flight (TOF) of scattered neutrons detected at position sensitive detectors (PSDs). The T_0 chopper was set at 50 Hz, a collimator of 1.5° was installed in front of the sample, and the "S" Fermi chopper with 200 Hz was used to obtain high neutron flux. We used a GM-type closed cycle cryostat to achieve 40 K and 15 K. The energy of the incident neutron beam was $E_i = 51.04$ meV yielding an energy resolution of $\Delta E = 2.5$ meV at the elastic position. We set the incident neutron beam with $\boldsymbol{k}_i // \boldsymbol{a}^*$.

3. Experimental results and discussions

An INS spectrum at 15 K is shown in Fig. 2(a). A well-defined flat excitation is observed at 17 meV and a weak flat one is observed at about 8 meV. Strong intensities at $\hbar\omega \lesssim 6$ meV in the wide Q range are from dispersive Fe-centered spin waves [14]. A weak flat intensity at about 20 meV is from an instrumental artifact [14]. Dispersive spectra in the range of $|Q| > 2$ Å^{-1} are from the aluminum that is used for the sample can and sample holder.

One-dimensional energy cuts obtained by integrating the intensities in the range of 1.5 Å^{-1} $\leq |Q| \leq$ 1.9 Å^{-1} are shown in Fig. 2(b). The red triangles and blue circles indicate the data measured at 40 K and 15 K, respectively. The data at 15 K are fitted by the sum of five Gaussian

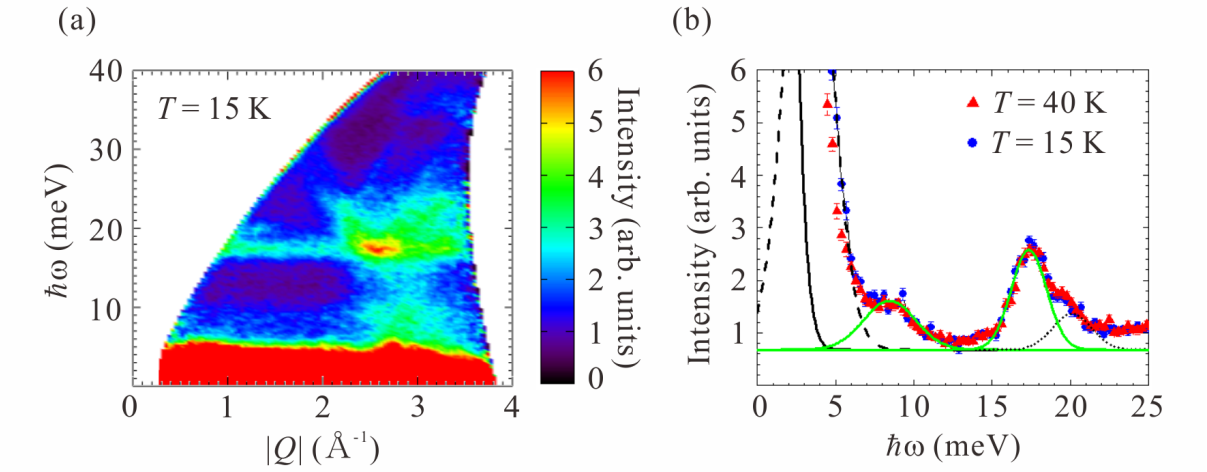

Figure 2. (a) An inelastic neutron scattering spectrum at 15 K. (b) $\hbar\omega$-dependences of the neutron intensities that are obtained by integration in the range of 1.5 Å$^{-1} \leq |Q| \leq$ 1.9 Å^{-1}. The triangles and circles are data at 40 K and 15 K, respectively. Solid, dashed and dotted curves are Gaussian fits to the data at 15 K.

functions; the solid black curve is for an incoherent elastic scattering, the dashed curve is for the Fe-centered spin-wave excitation, the solid green curve is for a couple of intrinsic excitations, and dotted curve is for the instrumental artifact. The peak energies of the green curve are estimated to be 8.5 meV and 17.4 meV, and they agree with the energy of the first and second excited states of the Nd^{3+} crystal field reported in the optical spectroscopy [11]. This suggests that these excitations are the transitions from the ground state to the first and second excited states. A quite small temperature dependence is observed between the data at 40 K and that at 15 K.

We simulated neutron intensities of the Nd^{3+} crystal field. At the Nd^{3+} site with the D_3 symmetry, the crystal field Hamiltonian is defined as follow:

$$\begin{aligned}\mathcal{H}_{\rm CF}(D_3) &= B_0^2 C_0^2 + B_0^4 C_0^4 + iB_3^4\left(C_3^4 + C_{-3}^4\right) \\ &\quad + B_0^6 C_0^6 + iB_3^6\left(C_3^6 + C_{-3}^6\right) + B_6^6\left(C_6^6 + C_{-6}^6\right). \end{aligned} \quad (1)$$

The B_q^p are the crystal field parameters and the C_q^p are the spherical tensor operators. We used the values of the parameters B_q^p reported in Ref. [11].

Then, the neutron intensity is expressed by

$$\frac{d\sigma}{d\Omega dE'} \propto \sum_{n,n'} p_n \left[\left|\langle n'|J_+|n\rangle\right|^2 + \left|\langle n'|J_-|n\rangle\right|^2\right] \delta\left(\hbar\omega + E_n - E_{n'}\right). \quad (2)$$

Here J_+ and J_- are, respectively, the raising and lowering operators of the total angular momentum $\boldsymbol{J}$, and p_n is the product of the probability that $|n\rangle$ state is occupied. E_n and $E_{n'}$ are the energies of the $|n\rangle$ and $|n'\rangle$ levels, respectively. We calculated the excitation energies and the neutron intensities of the transferred states from the ground state to the first and second excited states using *McPhase* software suit [19]. A ratio of the calculated intensities $(I_{\rm 1st}/I_{\rm 2nd})_{\rm cal}$ is 0.71, and that of the experimental intensities $(I_{\rm 1st}/I_{\rm 2nd})_{\rm exp}$ is 0.49. The experimental results are semi-quantitatively consistent with the calculations. Furthermore, we obtained the temperature dependence of the intensity as $(I_{\rm 40K}/I_{\rm 15K})_{\rm cal} = 0.93$ by calculating p_ns at 40 K and 15 K by assuming that the initial state was the ground state. The small temperature dependence is

consistent with the data in Fig. 2(b). The observed excitations are, thus, interpreted as the first and second excited states of the Nd^{3+} crystal field.

It is noted that the peak at 8.5 meV is broader than the peak at 17.4 meV in Fig 2(b). This broadening was also reported in the optical spectroscopy [11]. It is known that a spectrum of the crystal field excitation is broadened by coupling of phonon [20] and dynamic Jahn-Teller effect [21, 22]. This broadening of the peak is ascribed to an interaction between the Nd^{3+} moment and lattice vibration since the magnetoelastic coupling was observed in $NdFe_3(BO_3)_4$ [3].

4. Conclusion

The INS measurements were performed on the single crystals $NdFe_3(^{11}BO_3)_4$ to explore the Nd^{3+} crystal field excitations. In addition to the Fe-centered spin waves previously reported, dispersionless excitations are observed at 8.5 meV and 17.4 meV. Our analysis reveals that they are the transitions from the ground state to the first and second excited states of the Nd^{3+} ion in the crystal field.

Acknowledgments

We thank H. Matsuda, and K. Asoh for their contribution to the single crystal growth. The neutron scattering experiment was approved by the Neutron Scattering Program Advisory Committee of IMSS, KEK (Proposal No. 2013S01 and 2014S01). This work was supported by KAKENHI (24340077). S. Hayashida was supported by the Japan Society for the Promotion of Science through the Program for Leading Graduate Schools (MERIT).

References

[1] T. Kimura, T. Goto, H. Shintani, K. Ishizaka, T. Arima, and Y. Tokura, Nature (London) **426**, 55 (2003).
[2] A. K. Zvezdin, S. S. Krotov, A. M. Kadomtseva, G. P. Vorob'ev, Yu. F. Popov, A. P. Pyatakov, L. N. Bezmaternykh, and E. A. Popova, JETP Lett. **81**, 272 (2005).
[3] A. K. Zvezdin, G. P. Vorob'ev, A. M. Kadomtseva, Yu. F. Popov, A. P. Pyatakov, L. N. Bezmaternykh A. V. Kuvardin, and E. A. Popova, JETP Lett. **83**, 509 (2006).
[4] A. M. Kadomtseva, A. K. Zvezdin, A. P. Pyatakov, A. V. Kuvardin, G. P. Vorob'ev, Yu. F. Popov, and L. N. Bezmaternykh, JETP **105**, 116 (2007).
[5] A. K. Zvezdin, A. M. Kadomtseva, Yu. F. Popov, G. P. Vorob'ev, A. P. Pyatakov, V. Yu. Ivanov, A. M. Kuz'menko, A. A. Mukhin, L. N. Bezmaternykh, and I. A. Gudim, JETP, **109**, 68 (2009).
[6] A. M. Kadomtseva, Yu. F. Popov, G. P. Vorob'ev, A. P. Pyatakov, S. S. Krotov, and K. I. Kamilov, Low Temp. Phys. **36**, 511 (2010).
[7] U. Adem, L. Wang, D. Fausti, W. Schottenhamel, P. H. M. van Loosdrecht, A. Vasiliev, L. N. Bezmaternykh, B. Büchner, C. Hess, and R. Klingeler, Phys. Rev. B, **82**, 064406 (2010).
[8] A. I. Popov, D. I. Plokhov, and A. K. Zvezdin, Phys. Rev. B **87**, 024413 (2013).
[9] T. Kurumaji, K. Ohgushi, and Y. Tokura, Phys. Rev. **89**, 195126 (2014).
[10] N. Tristan, R. Klingeler, C. Hess, B. Büchner, E. Popova, I. A. Gudim, and L. N. Bezmaternykh, J. Magn. Magn. Mater. **316**, 621 (2007).
[11] M. N. Popova, E. P. Chukalina, T. N. Stanislavchuk, B. Z. Malkin, A. R. Zakirov, E. Antic-Fidancev, E. A. Popova, L. N. Bezmaternykh and V. L. Temerov, Phys. Rev. B **75**, 224435 (2007).
[12] P. Fischer, V. Pomjakushin, D. Sheptyakov, L. Keller M. Janoschek, B. Roessli, J. Schefer, G. Petrakovskii, L. Bezmaternikh, V. Temerov and D. Velikonov, J. Phys.:Condens. Matter **18**, 7975 (2006)
[13] M. Janoschek, P. Fischer, J. Schefer, B. Roessli, V. Pomjakushin, M. Meven, V. Petricek, G. Petrakovskii, and L. Bezmaternikh, Phys. Rev. B **81**, 094429 (2010).
[14] S. Hayashida, M. Soda, S. Itoh, T. Yokoo, K. Ohgushi, D. Kawana, H. M. Rønnow, and T. Masuda, Phys. Rev. B **92**, 054402 (2015).
[15] L. N. Bezmaternykh, S. A. Kharlamova, and V. L. Temerov Crystallogr. Rep. **49**, 855 (2004), translated from Kristallografiya, **49**, 945 (2004). Original Russian Text Copyright (c) 2004 by Bezmaternykh, Kharlamova, Temerov.
[16] S. Itoh, T. Yokoo, S. Satoh, S. Yano, D. Kawana, J. Suzuki, and T. J. Sato, Nucl. Instr. Meth. Phys. Res. A **631**, 90 (2011).
[17] S. Yano, S. Itoh, S. Satoh, T. Yokoo, D. Kawana, and T. J. Sato, Nucl. Instr. Meth. Phys. Res. A **654**, 421 (2011).

[18] S. Itoh, T. Yokoo, D. Kawana, H. Yoshizawa, T. Masuda, M. Soda, T. J. Sato, S. Satoh, M. Sakaguchi, and S. Muto, J. Phys. Soc. Jpn. **82**, SA033 (2013).
[19] M. Rotter, J. Magn. Magn. Mater. **272 − 276**, e481 (2004).
[20] E. T. Heyen, R. Wegerer, and M. Cardona, Phys. Rev. Lett. **67**, 144 (1991).
[21] S. Kern, C. Loong, J. Faber, and G. H. Lander, Solid State Commun. **49**, 295 (1984).
[22] A. T. Boothroyd, C. H. Gardiner, S. J. S. Lister, P. Santini, B. D. Rainford, L. D. Noailles, D. B. Currie, R. S. Eccleston, and R. I. Bewley, Phys. Rev. Lett. **86**, 2082 (2001).